PROCEEDINGS OF SPIE

SPIEDigitalLibrary.org/conference-proceedings-of-spie

Photoacoustic microscopy with 7.6-μm axial resolution

Chi Zhang, Konstantin Maslov, Junjie Yao, Lihong V. Wang

Chi Zhang, Konstantin Maslov, Junjie Yao, Lihong V. Wang, "Photoacoustic microscopy with 7.6-μm axial resolution," Proc. SPIE 8581, Photons Plus Ultrasound: Imaging and Sensing 2013, 85812W (4 March 2013); doi: 10.1117/12.2003248

SPIE.

Event: SPIE BiOS, 2013, San Francisco, California, United States

Photoacoustic microscopy with 7.6 μm axial resolution

Chi Zhang, Konstantin Maslov, Junjie Yao, and Lihong V. Wang*
Department of Biomedical Engineering, Washington *University in St. Louis, One Brookings Drive, St. Louis, MO 63130, USA*
* Corresponding author: LHWANG@WUSTL.EDU

ABSTRACT

The axial resolution of photoacoustic microscopy (PAM) is much lower than its lateral resolution, which resolves down to the submicron level. Here we achieved so far the highest axial resolution of 7.6 μm by using a commercial 125 MHz ultrasonic transducer for signal detection, followed by the Wiener deconvolution for signal processing. The axial resolution was validated by imaging two layers of red ink in a wedge shape. Melanoma cells were imaged *ex vivo* with high axial resolution. Compared with a PAM system with a 50 MHz ultrasonic transducer, our high-axial-resolution PAM system resolved the blood vessels in mouse ears *in vivo* much more clearly in the depth direction.

Keywords: photoacoustic microscopy, axial resolution, high-frequency ultrasonic transducer, deconvolution

1. INTRODUCTION

Photoacoustic microscopy has been demonstrated to image rich endogenous optical-absorption contrasts *in vivo*, including hemoglobin, melanin, DNA, RNA, cytochrome, myoglobin, bilirubin, water, and lipid.[1]–[8] At proper wavelengths, any molecules can potentially be imaged by PAM. Moreover, the functional parameters associated with these biomolecules can be imaged by PAM, such as hemoglobin oxygen saturation, blood flow speed, and temperature variation.[9]–[11] With these unique advantages, label-free PAM is expected to join the mainstream optical microscopy technologies.

Spatial resolution is a key parameter of microscopy. For optical-resolution (OR-) PAM, the lateral resolution, provided by the optical focusing, has achieved the submicron level in both transmission and reflection modes.[12],[13] The axial resolution, provided by the time-resolved ultrasonic detection, is limited by the ultrasonic transducer bandwidth[14] (approximately proportional to the central frequency). Since higher-frequency ultrasound attenuates faster in biological tissues, increasing the bandwidth for better axial resolution will decrease the maximum imaging depth. So far, ~15 μm axial resolution for depths up to 1.2 mm has been reported,[15],[16] but the axial resolution still remains much lower than the lateral resolution in OR-PAM.

Here we achieved so far the highest 7.6 μm axial resolution for PAM by using a commercial 125 MHz ultrasonic transducer for signal detection and the Wiener deconvolution method for signal processing. The high axial resolution was experimentally validated. As two example applications, we implemented high-axial-resolution imaging of melanoma cells *ex vivo* and mouse ears *in vivo*.

2. MATERIALS AND METHODS

Fig. 1 shows the high axial resolution PAM system. The laser (NT242-SH, Ekspla) generated laser pulses with a wavelength of 532 nm, a pulse width of 5 ns, and a repetition rate of 1 KHz. The laser pulses were focused onto the sample by a 0.32 NA objective, providing ~0.8 μm lateral resolution. The excited photoacoustic waves from the sample were detected by an ultrasonic transducer (125 MHz central frequency, 100 MHz bandwidth; V2062, Olympus NDT) with a focusing acoustic lens (0.8 NA). The photoacoustic signals were digitized at 1 GS/s and processed by a computer. The sample was mechanically scanned in 2D to generate a 3D image.

For each A-line signal, the envelope is normally extracted to convert the photoacoustic signal to a depth-resolved image. However, as shown in the literature, the axial (depth) resolution can be further improved by deconvolution methods.[13] The photoacoustic signal can be approximately modeled as the convolution of the system impulse response and the depth-resolved target function. Deconvolving the photoacoustic signal with the system impulse response helps to recover

Photons Plus Ultrasound: Imaging and Sensing 2013, edited by Alexander A. Oraevsky, Lihong V. Wang,
Proc. of SPIE Vol. 8581, 85812W · © 2013 SPIE · CCC code: 1605-7422/13/$18 · doi: 10.1117/12.2003248

the target function. In other words, deconvolution recovers the attenuated frequency components of the signal and broadens the system bandwidth, thereby improving the axial resolution (limited by the signal-to-noise ratio). Here the Wiener deconvolution method[17] was used to further enhance the axial resolution.

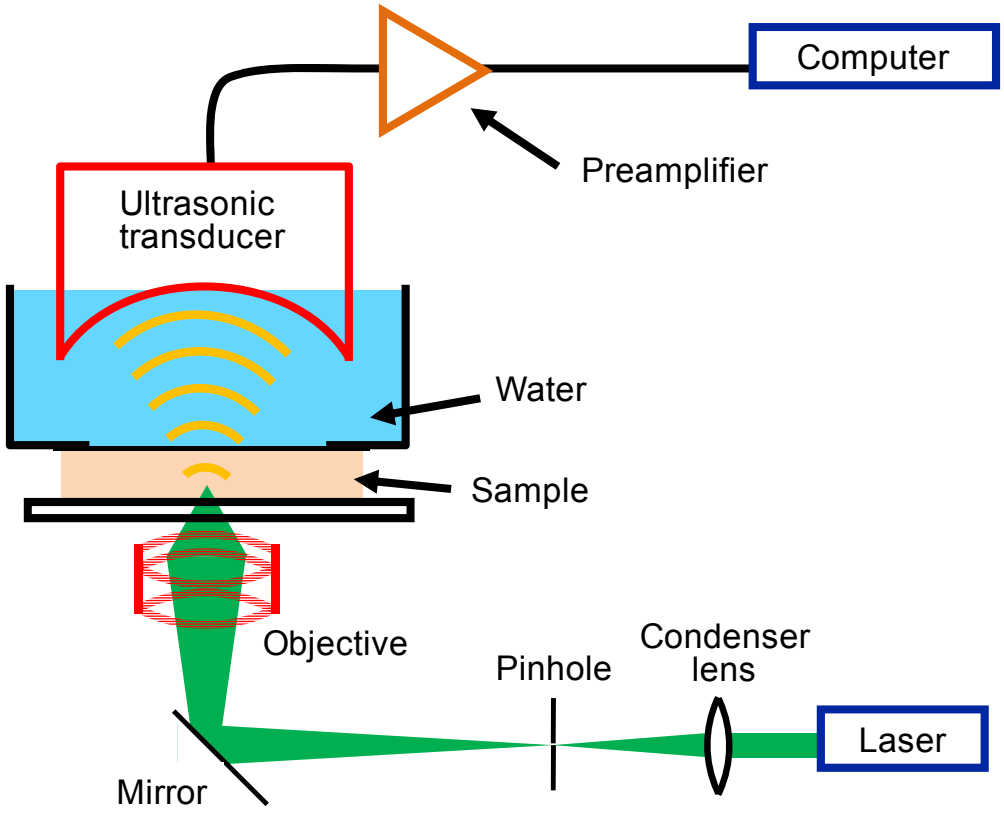

Figure 1. System schematic of PAM.

3. RESULTS AND DISCUSSION

We designed an experiment to quantitatively measure the axial resolution of the PAM system. The sample to be imaged is shown in Fig. 2(a). The sample consists of two layers of red ink, one on the polymethylpentene (TPX) plastic (upper) and the other on the glass slide (lower). The two layers were placed in a wedge shape, providing continuously variable distance between the two layers. The top layer was smeared on the TPX plastic because the acoustic impedance of the TPX plastic is close to that of water. A B-scan image of the sample calculated is shown in Fig. 2(b). The image was calculated by the deconvolution method to further improve the axial resolution. The contrast-to-noise ratio (CNR) versus the distance between the two layers was calculated. The axial resolution is defined as the distance with 6 dB CNR. It can be calculated that the axial resolution of the PAM system is 7.6 μm. Fig. 2(c) shows the profile across the B-scan image where the distance between the two layers is 7.6 μm.

We used the high-axial-resolution PAM system to image melanoma cells *ex vivo*. The cells were seeded onto a slide at a density of 30 mm^{-2} and fixed by formalin. The PAM image of a melanoma cell is rendered in 3D as a video (Video 3). The bright dots in the PAM images are melanosomes, the organelles containing melanin. The 3D structure of the cell was resolved in both lateral and axial directions. Note that here PAM generates a 3D image without depth scanning, which, however, is required in confocal microscopy and two photon microscopy.

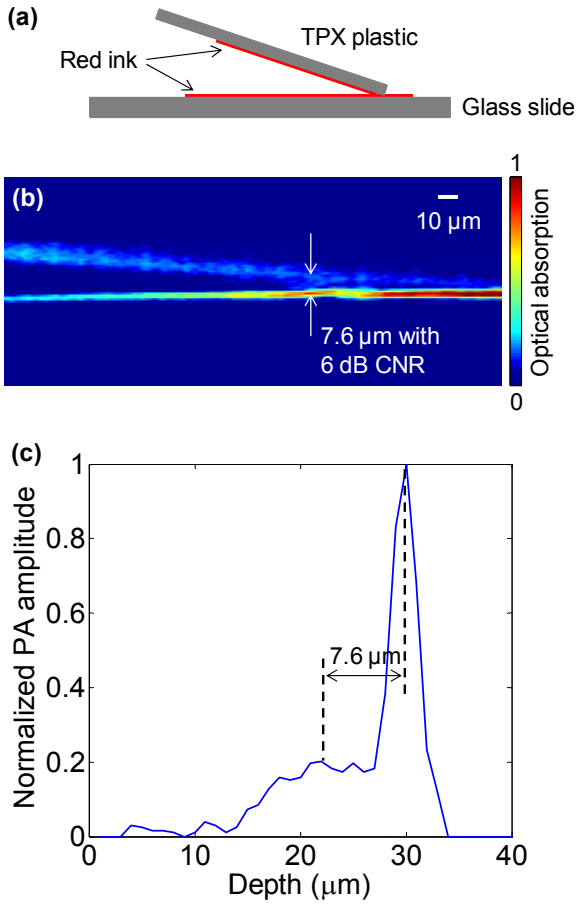

Figure 2. (a) The sample to be imaged consists of two layers of red ink in a wedge shape. (b) The B-scan image of the sample. (c) The profile across the B-scan image where the distance between the two layers is 7.6 μm.

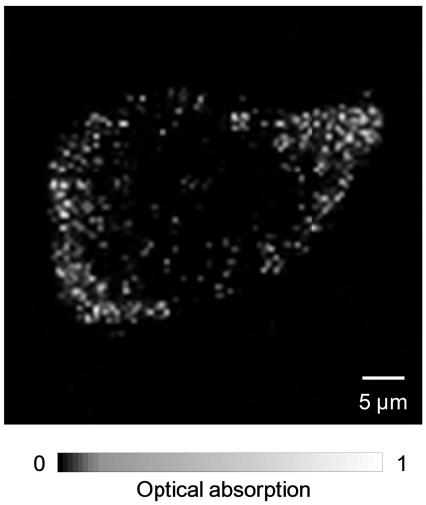

Video 3. 3D PAM image of a melanoma cell *ex vivo*. http://dx.doi.org/doi.number.goes.here

By imaging mouse ears *in vivo*, we compared the high-axial-resolution PAM with a PAM system[18] which uses a 50 MHz ultrasonic transducer (90% bandwidth). The system with the lower-frequency transducer also worked in transmission mode to provide a fair comparison. The difference between the two systems in axial resolution was expected to be >2 times. Figs. 4(a) and 4(b) show a pair of B-scan images of an ear at the same position from the two systems. Figs. 4(c) and (4d) show another pair of images. It can be seen that the blood vessels are resolved much more clearly by the high-axial-resolution PAM system with the 125 MHz ultrasonic transducer.

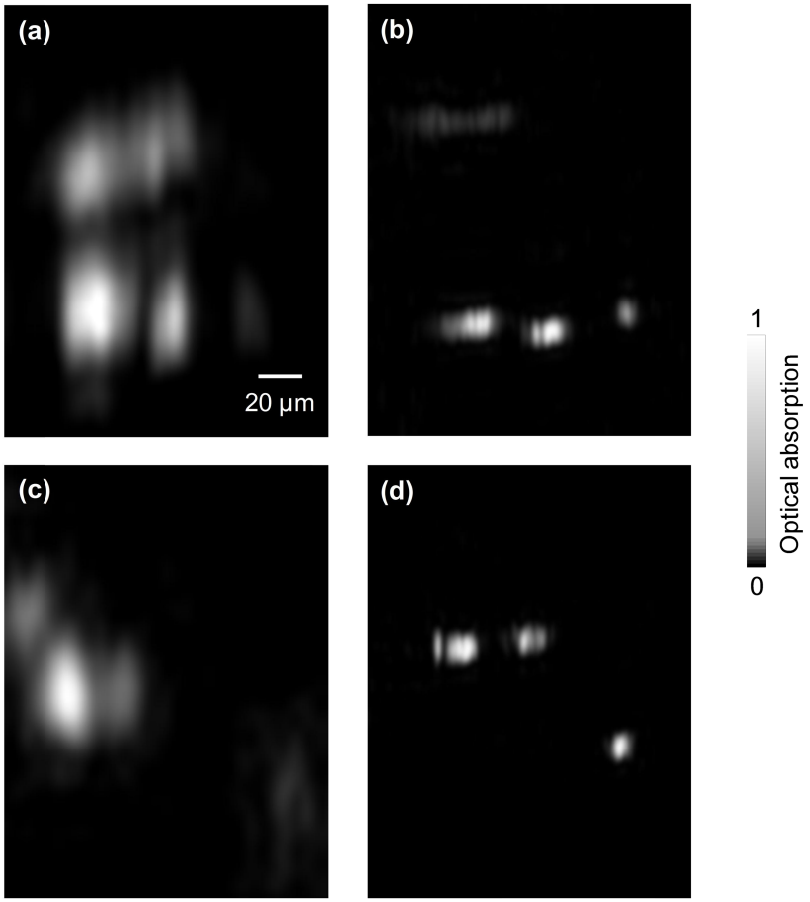

Figure 4. B-scan PAM images of a mouse ear *in vivo* acquired with (a,c) 50 MHz and (b,d) 125 MHz ultrasonic transducers.

We analyzed the detection sensitivity of our PAM system, which is a major concern when using a high-frequency ultrasonic transducer. In the *in vivo* mouse ear imaging experiment, the laser pulse energy was about 150 nJ, and the surface laser fluence was estimated to be 6.5 mJ/cm^2, well below the American National Standards Institute (ANSI) safety limit of 20 mJ/cm^2. So the 125 MHz ultrasonic transducer is suitable for *in vivo* blood vessel imaging. If we want to further improve the axial resolution by simply using a higher-frequency ultrasonic transducer, the penetration depth may be quite limited because in most soft tissues the attenuation coefficient is nearly proportional to the acoustic frequency.[19]

4. CONCLUSIONS

An axial resolution of 7.6 μm, the finest thus far, has been achieved for PAM. The results were validated by phantom experiments, *ex vivo* cell imaging and *in vivo* mouse ear imaging. The improved axial resolution benefits PAM in high-resolution 3D imaging.

The improvement of axial resolution was largely contributed by the deconvolution method. With higher SNR achieved by technology development, we expect to achieve an even better axial resolution. However, note that deconvolution should be applied to a linear and shift-invariant system. In PAM, the linearity holds well with low laser intensity while absorption saturation or nonlinear thermal expansion can be ignored.[20] The shift invariance holds accurately within the focal zone of the ultrasonic transducer.

ACKNOWLEDGMENT

This work was sponsored in part by National Institutes of Health grants R01 EB000712, R01 EB008085, R01 CA134539, U54 CA136398, R01 CA157277, and R01 CA159959. L.W. has a financial interest in Microphotoacoustics, Inc. and Endra, Inc., which, however, did not support this work. K.M. has a financial interest in Microphotoacoustics, Inc.

REFERENCES

[1] H. F. Zhang, K. Maslov, G. Stoica, and L. V. Wang, "Functional photoacoustic microscopy for high-resolution and noninvasive *in vivo* imaging," Nat. Biotech. 24(7), 848–851 (2006).
[2] D.-K. Yao, K. Maslov, K. K. Shung, Q. Zhou, and L. V. Wang, "*In vivo* label-free photoacoustic microscopy of cell nuclei by excitation of DNA and RNA," Opt. Lett. 35(24), 4139–4141 (2010).
[3] C. Zhang, Y. S. Zhang, D.-K. Yao, Y. Xia, and L. V. Wang, "Label-free photoacoustic microscopy of cytochromes," J. Biomed. Opt. 18(2), 020504 (2013).
[4] C. Zhang, Y.-J. Cheng, J. Chen, S. Wickline, and L. V. Wang, "Label-free photoacoustic microscopy of myocardial sheet architecture," J. Biomed. Opt. 17(6), 060506 (2012).
[5] Y. Zhou, C. Zhang, D.-K. Yao, and L. V. Wang, "Photoacoustic microscopy of bilirubin," J. Biomed. Opt. 17(12), 126019 (2012).
[6] Z. Xu, Q. Zhu, and L. V. Wang, "*In vivo* photoacoustic tomography of mouse cerebral edema induced by cold injury," J. Biomed. Opt. 16(6), 066020 (2011).
[7] H.-W. Wang, N. Chai, P. Wang, S. Hu, W. Dou, et al., "Label-free bond-selective imaging by listening to vibrationally excited molecules," Phy. Rev. Lett. 106(23), 238106 (2011).
[8] T. J. Allen, A. Hall, A. P. Dhillon, J. S. Owen, and P. C. Beard, "Spectroscopic photoacoustic imaging of lipid-rich plaques in the human aorta in the 740 to 1400 nm wavelength range," J. Biomed. Opt. 17(6), 061209 (2012).
[9] J. Yao, K. Maslov, Y. Zhang, Y. Xia, and L. V. Wang, "Label-free oxygen-metabolic photoacoustic microscopy in vivo," J. Biomed. Opt. 16(7), 076003 (2011).
[10] Y. Wang, K. Maslov, and L. V. Wang, "Spectrally encoded photoacoustic microscopy using a digital mirror device," J. Biomed. Opt. 17(6), 066020 (2012).
[11] J. Shah, S. Park, S. Aglyamov, T. Larson, L. Ma, et al., "Photoacoustic imaging and temperature measurement for photothermal cancer therapy," J. Biomed. Opt. 13(3), 034024 (2008).
[12] C. Zhang, K. Maslov, and L. V. Wang, "Subwavelength-resolution label-free photoacoustic microscopy of optical absorption *in vivo*," Opt. Lett. 35(19), 3195–3197 (2010).
[13] C. Zhang, K. Maslov, S. Hu, R. Chen, Q. Zhou, et al., "Reflection-mode submicron-resolution *in vivo* photoacoustic microscopy," J. Biomed. Opt. 17(2), 020501 (2012).
[14] C. Zhang, K. Maslov, J. Yao, and L. V. Wang, "*In vivo* photoacoustic microscopy with 7.6-μm axial resolution using a commercial 125-MHz ultrasonic transducer," J. Biomed. Opt. 17(11), 116016 (2012).
[15] L. Wang, K. Maslov, J. Yao, B. Rao, and L. V. Wang, "Fast voice-coil scanning optical-resolution photoacoustic microscopy," Opt. Lett. 36(2), 139–141 (2011).
[16] Y. Wang, K. Maslov, C. Kim, S. Hu, and L. V. Wang, "Integrated photoacoustic and fluorescence confocal microscopy," IEEE Trans. Biomed. Eng. 57(10), 2576–2578 (2010).

[17] J. A. Jensen, J. Mathorne, T. Gravesen, and B. Stage, "Deconvolution of in-vivo ultrasound B-mode images," Ultrason. Imag. 15(2), 122–133 (1993).
[18] J. Yao, K. Maslov, E. R. Puckett, K. J. Rowland, B. W. Warner, et al., "Double-illumination photoacoustic microscopy," Opt. Lett. 37(4), 659–662 (2012).
[19] P. T. Wells, Biomedical Ultrasonics, Academic Press, New York, pp. 120–123 (1977).
[20] A. Danielli, C. P. Favazza, K. Maslov, and L. V. Wang, "Picosecond absorption relaxation measured with nanosecond laser photoacoustics," Appl. Phys. Lett. 97(16), 163701 (2010).